Process Biochemistry 92 (2020) 138–148

Contents lists available at ScienceDirect

Process Biochemistry

journal homepage: www.elsevier.com/locate/procbio

In vitro and *in vivo* anticandidal efficacy of green synthesized gold nanoparticles using *Spirulina maxima* polysaccharide

S.H.S. Dananjaya[a], N.T. Thu Thao[a], H.M.S.M. Wijerathna[b], Jisoo Lee[a], M. Edussuriya[c], Dongrack Choi[a], R. Saravana Kumar[d,*]

[a] Zerone Bio Inc, 3 Floor, Sanhak Building, Dankook University, Dandae-ro 119, Dongnam-gu, Cheonan Si, Chungcheongnam-do, 31116, Republic of Korea
[b] Department of Aquaculture and Aquatic Resources Management, University College of Anuradhapura, Sri Lanka
[c] Department of Chemistry, Faculty of Science, University of Ruhuna, Matara, Sri Lanka
[d] Department of Physics, Periyar University Constituent College of Arts and Science, Idappadi, Salem 637102, Tamil Nadu, India

ARTICLE INFO

Keywords:
Gold nanoparticles
Green synthesis
Spirulina maxima
Antifungal activity
Candida albicans
Biocompatibility

ABSTRACT

This study, for the first time, demonstrated an unprecedented approach for the green synthesis of gold (Au) nanoparticles (NPs) using the polysaccharide of *Spirulina maxima* as a reducing agent. Time-kill kinetic analysis was used to evaluate the antifungal activity of the green synthesized Au NPs against the pathogenic *Candida albicans* (*C. albicans*). The minimum inhibitory concentration (MIC) and minimum fungicidal concentration (MFC) were found to be 32 μg/mL and 64 μg/mL, respectively. Ultra-structural analysis indicated prominent damage on cell wall of the *C. albicans* after Au NPs treatment, and suggested that the treatment could increase the membrane permeability and disintegration of cells leading to cellular death. The results of propidium iodide (PI) uptake assay showed the higher level of cell death in Au NPs treated *C. albicans* cells, further confirming the loss of plasma membrane integrity. Cytotoxicity analysis of Au NPs on HEK293T and A549 cells showed no cytotoxic effect up to 64 μg/mL of Au NPs concentration, indicating the potential use in *in vivo* studies. Also, the recovery of *C. albicans* infected zebrafish after Au NPs therapy suggest green synthesized Au NPs from *S. maxima* polysaccharide as a prospective anticandidal agent.

1. Introduction

Spirulina is a microscopic filamentous cyanobacteria, commercially cultivated as human food supplement and animal feed ingredient, because of its high amount of protein, polysaccharide, a variety of vitamins, essential fatty acids, carotene and minerals content [1,2]. Most commonly utilized species of genus *Spirulina* (*Arthrospira*) are *Spirulina platensis* (*S. platensis*) and *Spirulina maxima* (*S. maxima*) [1]. Polysaccharides are biomacromolecules formed by repeating monosaccharides units joined together by glycosidic bonds and exist as cell wall structural components in algae [3]. Polysaccharides isolated from *Spirulina* has been reported to possess antitumor, antioxidant, radio protective, immune regulative, antimicrobial, and anti-inflammatory activities [2,4–7]. The activities of *Spirulina* polysaccharide (*SP*) vary with the existing form and structure, and hence, its extraction method plays significant role in their activities.

In recent years, synthesis of metallic nanoparticles (NPs) for biomedical application using marine microorganisms was extensively studied [8]. Green synthesis of metal NPs using natural polysaccharides as stabilizing and reducing agents is considered promising field in nanotechnology [9]. Among the metal NPs, there are only a few reports of the synthesis of gold (Au) NPs using extracts of algae [10]. The Au NPs were synthesized using the extracts of green algae, such as *Chlorella pyrenoidusa* [11], *Pithophora oedogonia* [12], *Ulva fasciata* [13], cyanobacteria *S. platensis* [14] and *Plectonema boryanum* [15]. The Au NPs synthesized by cyanobacteria possessed unique physiochemical properties such as high surface to volume ratio, and wide optical and surface properties, which may help to interact with a broad range of microbes such as bacteria and fungi [10,14]. However, there are no reports yet on the synthesis of Au NPs using *S. maxima* polysaccharide.

Candida albicans (C. albicans) is the most dominant fungal species of the human microbiota and is asymptomatically colonized in the gastrointestinal and genitourinary tract of healthy people [16]. It is an opportunistic pathogen that can cause infections under certain pathological and physiological (immune compromised) conditions such as infancy, diabetes, pregnancy, steroidal chemotherapy, and prolonged broad spectrum antibiotic administration as well as acquired immunodeficiency syndrome (AIDS) [17]. The development of bacterial

* Corresponding author.
E-mail address: saravanakumarak@gmail.com (R. Saravana Kumar).

https://doi.org/10.1016/j.procbio.2020.03.003
Received 29 October 2019; Received in revised form 14 February 2020; Accepted 2 March 2020
Available online 03 March 2020
1359-5113/ © 2020 Published by Elsevier Ltd.

resistance has been studied exclusively over the last decade. However, there is less concern about the development of antifungal resistance. *C. albicans* have been observed for certain resistance levels and decreased activities in currently used antifungal drugs such as fluconazole, itraconazole, nystatin, caspofugin, ketoconazole, flucytosine and amphotericin B [18]. Previous studies have shown that such resistance might be the major cause of failure in the treatment of candidiasis [19]. Recently, the development of novel and effective antifungal agents such as antimicrobial peptides, plant extracts, metal and metal oxides NPs against *C. albicans* have gained considerable interest [20].

Therefore, in the present study, the easy green synthesis of Au NPs is reported using an aqueous solution of *SP* and gold (III) chloride trihydrate ($HAuCl_4{\cdot}3H_2O$) without the addition of any reducing agent. Ultrasonic treatment was used to breakdown the *S. maxima* cell wall and the polysaccharide extracted into acid hot water, followed by ethanol precipitation. The extracted *SP* was characterized by determining the total phenolic content, sugar composition and antioxidant activities on assay of DPPH radicals'. The synthesized Au NPs were used to investigate the *in vitro* antifungal activity against the pathogenic *C. albicans* using various parameters such as minimum inhibitory concentration (MIC), minimum fungicidal concentration (MFC), cell viability, and changes in cell membrane permeability. Also, the biocompatibility of Au NPs was analyzed using normal human embryonic kidney (HEK293T) and human lung adenocarcinoma epithelial (A549) cells. Besides, the *in vivo* antifungal activity of Au NPs was tested using zebrafish infection model and the anticandidal activity of Au NPs in zebrafish muscle was further analyzed by histopathological analysis and host immune responses. It should be emphasized here that this is the first report on the anticandidal activity and biocompatibility of Au NPs synthesized using *SP*.

2. Materials and method

2.1. Extraction of polysaccharides from S. maxima

The dried powder form of pure culture of *S. maxima* was generously supplied by Emem exports, Chennai, India. Polysaccharides were extracted from S. maxima using ultrasonic disruption coupled with hot water extraction method with some modifications [21,22]. Briefly, 6 *g* of freeze dried *S. maxima* powder was mixed with 120 mL of demineralized acid water (pH = 2.5). The resulting mixture was exposed to ultrasonic treatment in ultra-sonication bath (LP-XP 250, labCAN, China; ultrasonic power 60 W) at a temperature of 90 °C for 2 h, centrifuged at 5000 rpm for 30 min and the supernatant was collected. Then, 95 % ethanol and the supernatant were mixed together in a 4:1 ratio and the mixture was stored at a temperature of 4 °C for 12 h. Thereafter, the polysaccharide was precipitated by centrifugation at 8000 rpm for 30 min. The precipitate was washed stepwise with saturated sodium acetate in 95 % ethanol, and absolute ethanol, and dried in an oven at 50 °C to obtain constant weight. Finally, the dry weight was measured to calculate the percentage polysaccharides extraction yield (%) using the formula,

The polysaccharides extraction yield % (w/w) = W_0/W

Where, W_0 (g) is the weight of dried *SP*, and W (g) is the weight of dried powder of *S. maxima*.

2.2. Determination of sugar compositions in SP

Analysis of sugar content was performed by gas chromatography (GC 17A, Shimadzu, Japan) as described in Ref. [22]. Monosaccharides were obtained by mixing 10 mg of sample and 1 mg of internal standard (myo-inositol; Sigma), followed by hydrolysis using 2 N sulfuric acid at a temperature of 100 °C for 8 h. The sample was allowed to cool after which barium carbonate ($BaCO_3$) was added and the mixture was filtered. For preparation of the sugar derivatives alditol acetates, 1 mL of sodium tetraborohydride (20 g/L) was added to the filtrate. After standing overnight at 4 °C, the solution was filtered and evaporated. The sample was then treated with 0.5 mL of acetic anhydride and 0.5 mL of pyridine and kept at a temperature of 80 °C for 2 h. After cooling, the sample was mixed with 1 mL of methanol and evaporated. The residue was treated with 1 mL of heptane, evaporated to dehydration and re-dissolved in dichloromethane. Finally, the sugar content in the sample was determined using GC with a capillary column (0.25 mm × 30 m, Rtx-2330) at a temperature of 220 °C, with injector and flame ionization detector (FID) at a temperature of 230 °C. Identification of sugar composition was done by co-chromatography with authentic standards (Sigma, USA.). The percentages of monosaccharides in the samples were calculated by the peak areas of the graph.

2.3. Determination of total phenolic content in SP

Phenolic content of *SP* was determined by using the Folin-Ciocalteau's phenol reagent as described in Ref. [23] with some modifications. Briefly, 100 µL of the sample was collected in individual test tubes and the blank was prepared with 100 µL of H_2O. Then, 2 mL of 2% sodium carbonate was added to each tube and left in dark at 25 °C. After 2 min, 100 µL of 50 % Folin-Ciocalteu's phenol reagent was added to each tube and incubated in the dark at 25 °C for 30 min until the color of the reaction mixture changed from yellow to blue. A total of 200 µL from each test tube was transferred to a 96-well microplate and the absorbance was measured at 720 nm, using a microplate reader. Quantification was done considering the standard curve for gallic acid (20 − 100 µg/mL).The results were given as milligrams of gallic acid equivalents (mg GAE) per gram of dry sample.

2.4. Antioxidant activity of polysaccharides

Investigation of antioxidant activity of *SP* was carried out by 1,1-Diphenyl-2-picrylhydrazyl free radical (DPPH•) scavenging activity assay. DPPH• scavenging activity assay was done to determine the antioxidant activity of extracted *SP* according to Ref. [24] with some modifications. Briefly, 0.1 mM DPPH and 2.5 mg/mL *SP* solutions were prepared in ethanol and water, respectively. Then, 1 mL of *SP* solution with different concentrations (50-300 µg/mL) was added to the tubes, holding 5 mL of DPPH solution. The mixture was vortexed and subsequently incubated in the dark at a temperature of 37 °C for 30 min. Finally, the absorbance was taken at 517 nm to calculate the ability to scavenge the DPPH radical (%).The calculation was done according to the equation given below [22],

$$\text{Scanvenger rate } (\%) = \left(1 - \frac{A\ sample}{A\ control}\right)$$

Where, $A_{control}$ and A_{sample} are the absorbance of the control and the absorbance of the samples, respectively. Butylated hydroxytoluen (BHT, Sigma, USA) was used as the positive control.

2.5. Preparation and characterization of Au NPs using SP

The Au NPs were synthesized according to the method described in Ref. [25] with slight modifications. Briefly, 5 mg/mL of *SP* and 4 mM of $HAuCl_4{\cdot}3H_2O$ solutions were prepared using Milli-Q (Millipore) water. 10 mL of *SP* solution was mixed with 2 mL of $HAuCl_4{\cdot}3H_2O$ solution and the mixture was heated in a water bath at 90 °C for about 5 min until the color change occurred from pale yellow to purple red, indicating the formation of Au NPs.

Spectrophotometer (Mecasys, Korea) was used to record the UV–vis absorption spectra of Au NPs in the wavelength range of 325 − 600 nm. Transmission electron microscopy (TEM, Tecnai G2 F-20, FEI, USA) was

used to characterize the general morphology of the synthesized Au NPs with an operating voltage of 300 kV. Zetasizer S-90 Malvern instruments (Malvern, UK) was used to determine the distribution of the particle size and zeta potential. X-ray diffraction of Au NPs was carried out using a XRD diffractometer (D8-Advance, Bruker, USA).

2.6. Growth conditions of C. albicans

C. albicans KCTC 27,242, was purchased from the Korean Collection for Type Culture. A single colony was carefully picked from fresh potato dextrose agar (PDA) plate and transferred into potato dextrose broth (PDB) to enable growing under aerobic condition in a shaking incubator operating at 180 rpm and at 30 °C for 24 h. Pelletizing of *C. albicans* cells were done by centrifugation at 3500 rpm for 10 min. Then the cell pellet was washed twice with phosphate buffered saline (PBS, pH ~ 7.4) and re-suspended in PBS (OD_{600} = 0.1) to adjust the final concentration of 10^6 colony forming units per milliliter (CFU/mL). Calculation was performed using a hemocytometer.

2.7. Determination of minimum inhibitory concentration (MIC)/minimum fungicidal concentration (MFC) of Au NPs and it's in vitro zone of inhibition

Evaluation of antifungal effect of Au NPs on *C. albicans* was performed using broth microdilution susceptibility test as described in our previous study [26]. The antifungal effect of Au NPs was tested with various concentrations ranging from 0 to 64 μg/mL and Nystatin (10 μg/mL) was used as the standard antifungal compound. The minimal concentration of Au NPs which can inhibit the growth of *C. albicans* was determined as MIC. MFC was determined by collecting 100 μL of the medium from wells and sub-cultured on PDA plates to investigate fungal growth after 24 h. The MFC indicates the lowest concentration which shows no microscopic growth on agar plates after 24 h. The determination of fungistatic or fungicidal effect of Au NPs was done by calculating the MFC/MIC ratio with MFC/MIC ≥ 4 as fungistatic and MFC/MIC < 4 as fungicidal.

The *in vitro* zone of inhibition of Au NPs was found by Agar disc diffusion method for the Clinical and Laboratory Standards Institute. Briefly, 10 μL of Au NPs with concentration 32 and 64 μg/mL was added on Whatman® filter paper disc (Qualitative, 20 − 25 μm pore size, 6 mm), soaked, and dried at room temperature. Then, 100 μL of each *C. albicans* isolates were separately swabbed in three directions on PDA medium. The inoculated Whatman paper discs were placed on the agar surface, incubated at a temperature of 35 °C for 48 h. Finally the diameter of the inhibition zone measured.

2.8. Time-kill kinetic analysis

C. albicans (10^6 CFU/mL) was incubated with different concentrations (4 − 32 μg/mL) of Au NPs in PDB at a temperature of 30 °C. The growth level of *C. albicans* at different time points after incubation (0, 3, 6, 9, 12, 15, 18, and 21 h) was examined by assessing the absorbance at 600 nm [26]. The positive control was incubated with Nystatin (10 μg/mL). All time-kill curve experiments were performed in triplicate.

2.9. Determination of the viability of C. albicans after Au NPs treatment

The viability of *C. albicans* upon the treatment of Au NPs was investigated by MTT assay. *C. albicans* (10^6 CFU/mL) culture was treated with various concentrations of Au NPs (8, 16, 32, 64 μg/mL) for 24 h. Then, the culture was pelletized by centrifugation at 3500 rpm for 10 min and the cell pellet was washed with PBS. The cell viability assessment was performed by reacting cells with 20 μL of MTT (5 μg/mL) (3-(4,5-dimethyl-2-thiazolyl)-2, 5-diphenyl-2H-tetrazolium bromide, Sigma Aldrich, USA) solution for 30 min. Thereafter, re-suspension of the samples were done by using dimethyl sulfoxide (DMSO, Sigma Aldrich, USA), and the cell viability was assessed by determining the OD value at 570 nm using a microplate reader (Bio- Rad, USA).

Table 1
Primers used in this study.

Gene name	Primers	NCBI Accession No.
Tumor necrosis factor- α (tnf-α)	F:AGAAGGAGAGTTGCCTTTACCGCT R: ACACCCTCCATACACCCGACTTT	AY427649
Interleukin-1β (il-1β)	F:TCAAACCCCAATCCACAGAG R: TCACTTCACGCTCTTGGATG	AY340959.1
Interleukin-6 (il-6)	F: TCAACTTCTCCAGCGTGATG R: TCTTTCCCTCTTTTCCTCCTG	JN698962.1
Interleukin-12 (il-12)	F: CTCAGGGAAACAGGATTACGG R: GATCTTCCTAAAGCTCCACTGG	AB183002.1
Interferon (ifn)	F: AAGGTGGAGGACCAGGTGAAGTTT R: GGCTTTGCGTATCTTGCCACACAT	AB093588.1
Chemokine ligand 18 b (cxcl18 b)	F: CTGCTGCTCGCGGTAGTTTA R: TCAACTTTGTCGCAGTTTGG	NM_001115060.1

2.10. Analysis of morphological changes of C. albicans after Au NPs treatment

C. albicans cells (10^6 CFU/mL) were treated with Au NPs (32 μg/mL) for 24 h. Then, the cells were pelleted and washed with PBS, followed by pre-fixation with 2.5 % glutaraldehyde for 30 min. The cells were washed again with PBS and dehydrated through a series of ethanol solution (30 %, 50 %, 70 %, 80 %, 90 %, 100 %). After the fixation, the cells were allowed to dry and then coated with platinum using ion sputter (E-1030, Hitachi, Japan), followed by observation using field-emission scanning electron microscopy (FESEM, SEISS SIGMA 500, SEISS, Germany). FESEM coupled with energy-dispersive X-ray spectroscopy (EDX, Thermo, Noran system7) was used to confirm the quantitative chemical composition of untreated and Au NPs treated *C. albicans* cell membranes.

2.11. Analysis of the effect of Au NPs on membrane permeability of C. albicans

Changes of the membrane permeability were determined by using propidium iodide (PI) uptake assay. The control and Au NPs treated *C. albicans* (at MIC and MFC levels) cell cultures were centrifuged (5000 rpm for 2 min). The cell pellets were washed and re-suspended in PBS. Next, the cell suspensions were incubated with 5 μg/mL of PI (Sigma Aldrich, USA) in the dark at a temperature of 30 °C for 15 min, and the cell suspension was washed twice to remove over staining. Lastly, single drop of each cell suspensions was positioned on a cover slip and fluorescence images were taken by Carl Zeiss LSM 5 Live confocal laser scanning microscope (CLSM) scan head, integrated with the Axiovert 200 M inverted microscope (Carl Zeiss, Jena, Germany).

2.12. Safety assessment of Au NPs

Toxicity level of Au NPs was evaluated using zebrafish (*in vivo*) and mammalian cells (*in vitro*). First, the toxicity of Au NPs was investigated using adult zebrafish *via* bath exposure administration. For achieving lethal concentration (LC_{50}) of Au NPs, the guidelines of Organization for Economic Cooperation, and Development (OECD) for testing the chemicals was adopted [27]. Briefly, different concentrations of Au NPs (12.5, 25, 50, 75, 100, and 125 mg/L) suspensions were exposed to the treatment group containing six zebrafish for 96 h in a 2 L tank containing 1 L of test solution. Each treatment was run in triplicates under the same conditions and the number of dead fishes from each treatment group was recorded at every 12 h and then immediately removed from the treatment group to avoid contaminations.

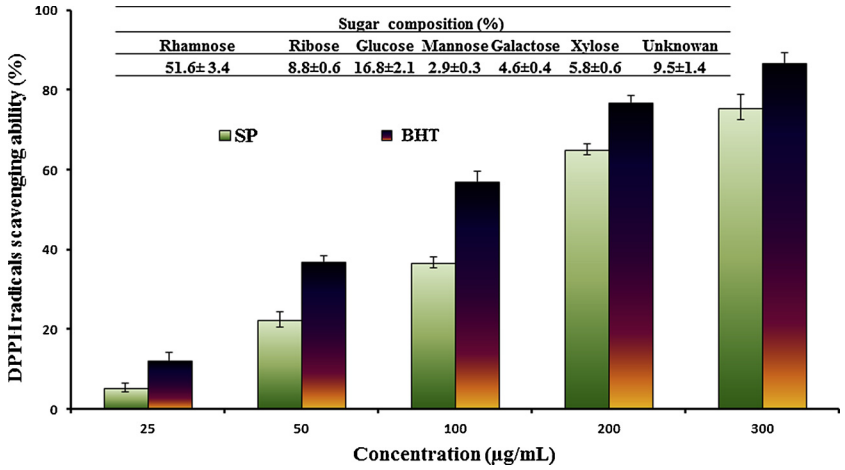

Fig. 1. Sugar composition of *SP* and scavenging effect of different *SP* concentrations (25, 50, 100, 200 and 300 µg/mL). *SP* on DPPH radicals compared with that of BHT. The bars indicate the mean ± SD. (n = 4).

The *in vitro* cytotoxicity was assessed using a standard MTT colorimetric method [28]. To determine the cytotoxic level, HEK293T (human embryonic kidney, ATCC-11268) and A549 (human lung adenocarcinoma epithelial, ATCC-185) cells were supplemented with Dulbecco's modified Eagle's medium (DMEM, Invitrogen, USA) with 1% antibiotic/antimycotic solution (Glibco, USA) and 10 % fetal bovine serum (FBS) (Hyclone, USA) which were grown in a humidified atmosphere (at 37 °C with 5% CO_2). Cells were seeded at a density of 1×10^4 cells/well in 96-well tissue culture plates. After 24 h, the cells were treated with different concentrations (0 − 128 µg/mL) of Au NPs. After 24 h treatment, 20 µL of MTT solution (5 mg/mL in PBS, pH = 7.4) was added to each well and after 4 h of incubation at 37 °C, the medium was removed and formazan crystals were solubilized with 200 µL of DMSO. The resulting solution was vigorously mixed to dissolve the reacted dye. After 15 min., optical density (OD) values for each well were measured at 570 nm using a microplate reader (Bio-Rad, USA). Cell viability was expressed relative to untreated cell cultures. Each experiment was performed using three replicates for each concentration.

2.13. In vivo efficacy of Au NPs upon C. albicans infection in zebrafish model

Wild type zebrafish (0.35 ± 0.05 g) were used in this study. Standard culture conditions were used to maintain the fish stock according to the guidelines previously described [29]. Antifungal activity of Au NPs upon *C. albicans* infection was verified using the zebrafish model according to the method described in our previous study [28]. Briefly, 90 zebrafish were divided equally into three groups with 3 replicates (n = 30/replicate). Zebrafish were anesthetized by immersing in 0.17 g/mL of tricaine (Sigma, USA) solution. Then, all the fish were injected with 3 µL of cells at the dose of 3×10^6 cell per fish by using Hamilton® syringe and fish were immediately transferred to recovery tanks (4 L). At 12 hpi, fish were anesthetized and 3 µL/fish of PBS, 32 µg/fish of Au NPs and 10 µg/fish of Nystatin were applied to the control, Au treatment and positive control groups, respectively. At every 12 h, the same procedure was carried out until 120 hpi cumulative mortality was measured throughout the period. Besides, histological analysis was done to examine the infection in zebrafish at 72 hpi. For this purpose, overdose of tricaine was used to euthanize three fish and were fixed in 10 % neutral buffered formalin for 24 h. Then, fish were washed with 1 x PBS for 12 h and decalcification was done by transferring the fish into 50 mL/fish of decalcifying solution Lite (Sigma, USA) for 3 days. Thereafter, fish was washed with 1 x PBS for 12 h. The infected sites were separated and processed for 12 h in tissue processor (Leica® TP1020 Semienclosed Benchtop Tissue Processor, Germany), followed by embedding in paraffin (Leica® EG1150 Tissue Embedding Center, Germany). The samples were then prepared into 4 µm thick sections using microtome (Leica® RM2125 microtome, Germany). Identification of the fungus in the tissue was done by staining serial transverse tissue sections with Periodic Acid-Schiff stain (PAS). The investigation of the samples was done by light microscope (Leica® 3000 LED, Germany). The images were taken by Nikon eclipse 80i (Nikon Corporation, Japan)

2.14. Transcriptional response of immune gene in zebrafish upon C. albicans infection

Fish in each treatment group were sacrificed at 72 hpi by immersion in tricane overdose and infected site dorsal muscle was separately isolated. Tissues collected from three fish were pooled, RNA was extracted using RNeasy Mini Kit (Qiagen, Seoul, Korea), and cDNA was synthesized using reverse transcriptase (Toyobo, Japan). Transcriptional levels of TNF-α, IL- 1β, IL-6, IL-12, INF-γ and Cxcl18b genes at 72 hpi were analyzed by Quantitative polymerase chain reaction (qPCR) using QuantiTect SYBR Green PCR kit (Qiagen) on a Rotor-Gene Q (Qiagen) and β-actin was used as the reference gene for normalization. Briefly, 4 µL of cDNA from each sample were separately mixed with 5 µL of 2x TaKaRa Ex-Taq™ SYBR premix and 0.5 µL of each forward and reverse primers. Initiation of the qRT-PCR cycling commenced with 30 s denaturation at 95 °C. Then, 40 cycles, with 5 s denaturation at 95 °C was done for the three-step thermal cycling process. Annealing was performed for 10 s at 55 °C followed by 20 s extension at 72 °C. After completion of 40 cycles dissociation curves were taken within the time of temperature increasing from 60 to 95 °C in order to check the compatibility of primer template. The expression fold calculation was done according to the $2^{-\Delta\Delta CT}$ [30]. Table 1 presents the specific primer pairs for each gene.

2.15. Statistical analysis

All the data related to the cell viability were illustrated as means ± SD for triplicate reactions. Statistical analysis was performed using unpaired, two-tailed *t*-test to calculate the *P*-value using GraphPad program ver. 6 (GraphPad Software, Inc.). The significant difference was defined at $P < 0.05$.

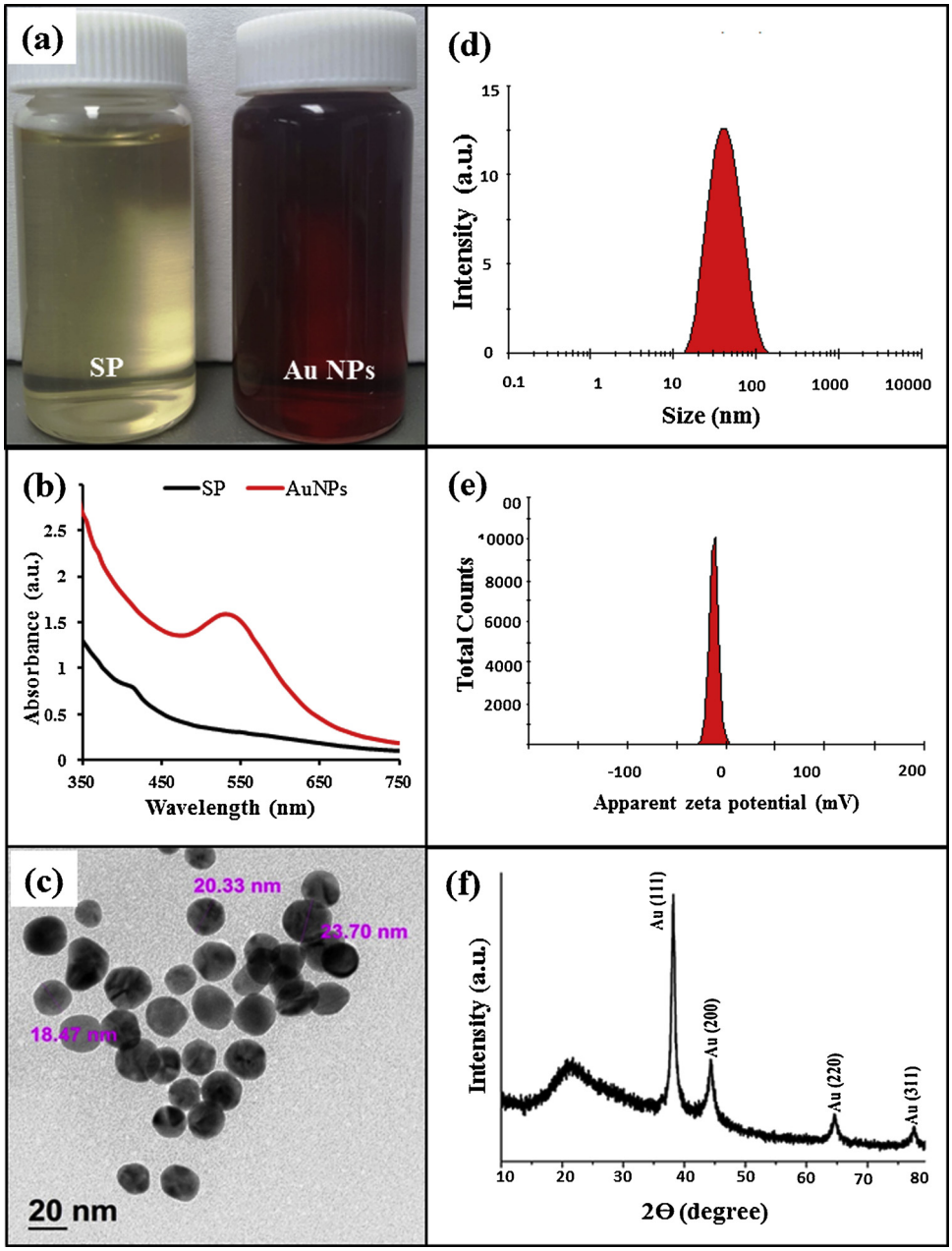

Fig. 2. Physio-chemical characteristics of Au NPs. (a) *SP* and Au NPs solutions; (b) UV–vis spectrum of *SP* and Au NPs; (c) TEM image of Au NPs; (d) Particle size distribution of Au NPs; (e) Zeta potential of Au NPs; (f) XRD spectrum of Au NPs.

3. Results and discussion

3.1. Characterization of S. maxima polysaccharides

In the present study, the polysaccharide from *S. maxima* was extracted by acid water extraction method, and the yield of the extracted *SP* was found to be 18.25 ± 3.4 %. The extracted *SP* was subjected to sugar composition analysis, and the GC result showed that the hydrolyzed polysaccharide consisted of six neutral sugars namely, rhamnose, ribose, glucose, mannose, galactose, and xylose with the composition of 51.6 ± 3.4 %, 8.8 ± 0.6 %, 16.8 ± 2.1 %, 2.9 ± 0.3 %, 4.6 ± 0.4 %, and 5.8 ± 0.6 %, respectively. There is also unknown polysaccharide with a composition of 9.5 ± 1.4 %. The major monosaccharides of *SP* which was isolated from *S. platensis* were rhamnose (24.7 %), glucose (16.15 %), and galactose (13.32 %) [31]. Similar glucose composition with different quantities was reported for the polysaccharide extracted using *Spirulina SP* [22,32]. The phenolic compounds in algae were proven to have potential antioxidant activity in algal polysaccharides [22]. The total phenolic content of *SP* was found to be 41.48 ± 2.56 mg GAE/g in the sample. Also, the DPPH scavenging activity of *SP* (Fig. 1) was analyzed at various concentrations (25, 50, 100, 200, and 300 µg/mL). The results indicated that DPPH scavenging activity of *SP* increases with increasing *SP* concentration similar to BHT (positive control). Similar scavenging pattern has been observed in earlier report [2].

3.2. Characterization of Au NPs

Conventional chemical reduction methods generally use harmful thiols and sodium borohydride as reducing agents for the synthesis of Au NPs. Green synthesis of Au NPs is highly recommended because it is simple, cost-effective, ecofriendly and a single step process [33,34].

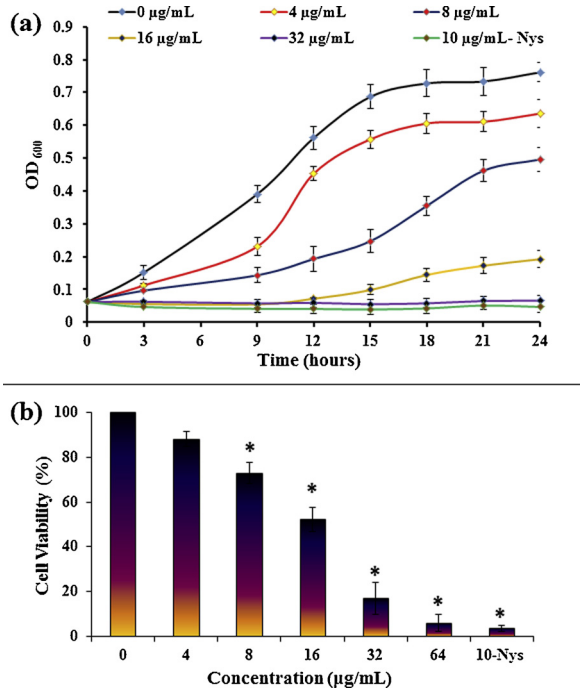

Fig. 3. Growth performance and cell viability of *C. albicans* exposed to different concentrations of Au NPs. (a) Cell growth assessed after treatment with Au NPs at 30 °C by the growth inhibition assay, which was measured as turbidity (OD 600 nm) for 24 h at 3 h intervals using microplate reader. The bars indicate the mean ± SD (n = 4). (b) Cell viability assessed after treatment with different concentrations of Au NPs. The asterisk (*) symbol indicates that mean values are significantly different ($p < 0.05$) between the treatment and the control.

Marine carbohydrates such as fucoidan, agarose, carrageenan and chitosan oligosaccharide have been used to synthesis Au NPs [35,36]. Herein, we used *SP* as a reducing and capping agent for the green synthesis of Au NPs. The color of the *SP* solution (pale-yellow) transformed to ruby-red after the addition of $HAuCl_4{\cdot}3H_2O$ into the *SP* solution (Fig. 2(a)). This color change occurred due to the excitation of surface plasmon resonance (SPR) in the Au NPs [37]. The UV–vis absorption spectrum (Fig. 2(b)) displayed different absorption profiles for *SP* and Au NPs. The *SP* solution did not show any notable peak between the wavelength ranges of 325 − 600 nm while the Au NPs exhibited a clear absorption peak at 530 nm. This strong absorption band observed at 530 nm was due to the excitation of SPR, which depends on the size, shape, and dispersion of Au NPs [38].

The size of the NPs play an important role in the determination of the antimicrobial activity due to their penetration ability into the eukaryotic cells *via* active or passive uptake pathways [39]. The TEM image (Fig. 2(c)) showed spherical and highly polydispersed Au NPs with 16 − 23 nm size. The average particle size distribution of Au NPs (Fig. 2(d)) was 36.45 ± 3.25 nm. The slightly high diameter of the Au NPs was attributed to the stationary layer of fluid attached to the particles. Therefore, the actual particle size should be lower than the value given by Zetasizer S-90 analyzer. Zeta potential values basically show the stability of the particles which prevents the aggregations in aqueous solution. The zeta potential value of Au NPs was found to be -12.25 ± 2.35 mV (Fig. 2(e)), which is consistent with the zeta potential of −24.1 mV for Au NPs described previously [40]. The XRD pattern of Au NPs (Fig. 2(f)) showed major diffraction peaks at 38.14°, 44.49°, 64.56° and 77.45° corresponding to the (111), (200), (220) and (311) crystalline planes of face centered cubic (FCC) structure of Au, respectively (JCPDS card no. 04-0783). The broad hump at 20.33° corresponds to the amorphous *SP*. Similar amorphous peak was observed in the polysaccharide extracted from *S. platensis* [32]. The mean crystallite size of Au NPs calculated using Debye-Scherrer equation was found to be 16.25 nm, which is consistent with the value obtained from TEM analysis. The strong antioxidant activity of water soluble *SP* triggered the reduction of Au cations in the NPs synthesis, which is consistent with the results of previous studies with phenolic antioxidants that are responsible for the reduction of Ag and Au NPs [41].

3.3. Effects of Au NPs on the growth and cell viability of C. albicans

The MIC and MFC of the synthesized Au NPs against *C. albicans* were found to be 32 µg/mL and 64 µg/mL, respectively. The MFC/MIC ratio was used to determine whether the substance had fungistatic (MFC/MIC ≥ 4) or fungicidal (MFC/MIC ≤ 4) activity [42]. The MFC/MIC ratio of 2 was obtained for our green synthesized Au NPs, suggesting the fungicidal activity against *C. albicans*. The *in vitro* zone of inhibition by disc diffusion method for the Au NPs treated *C. albicans* at the MIC and MFC levels were found to be 11.5 ± 0.2 mm and 16.3 ± 0.3 mm, respectively

Growth inhibition of *C. albicans* by Au NPs was tested by means of time-kill kinetic analysis. Cell growth was determined after the treatment with Au NPs for different concentrations (0, 4, 8, 16 and 32 µg/mL). Experimental results (Fig. 3(a)) demonstrated that increasing the Au NPs concentration reduced the growth performance of *C. albicans* compared to the control. At MIC level (32 µg/mL), the growth inhibition effect was almost similar to the positive control (10 µg/mL), indicating no cell growth over time. Also at 4, 8, and 16 µg/mL of Au NPs substantial reduction in the *C. albicans* cell number was observed when compared to the positive control. Only few studies have been conducted to evaluate the anticandidal activities of green synthesized Au NPs and their mode of action. It was stated that commercially available Au NPs with 30 nm diameter exhibit growth inhibitory effect on *C. albicans* with the same MIC level (32 µg/mL) [43]. Similarly, Au NPs conjugate-methylene blue had 31.2 and 62.5 µg/mL of MIC and MFC, respectively [44]. According to the result of E.D. Alteriis et al., indolicidin conjugated Au NPs had MIC values that ranged from 150 to 200 µg/mL against several strains of *C. albicans,* and the MFC values ranged from 150 to 300 µg/mL [16]. The amino acid of *C. albicans* can be conjugated with triangular Au NPs through thiol-gold interaction [45]. This interaction is useful to inactivate the activity of sap enzyme which is a key virulent factor of *C. albicans* [46]. Further studies are needed to investigate the mode of action of green synthesized Au NPs.

MTT assay was performed to examine the cell viability of *C. albicans* treated with Au NPs for different concentrations (0, 4, 8, 16, 32, and 64 µg/mL). Results (Fig. 3(b)) showed clear impact of Au NPs on the cell viability of *C. albicans.* Increasing the concentrations of Au NPs caused significant cell death ($p < 0.05$), and at the MIC level (32 µg/mL) the cell viability was found to be 17 %, which further decreased to 6% for 64 µg/mL. The cell viability for the positive control (Nystatin) at 10 µg/mL was 3.6 %.

3.4. Effects of Au NPs on the morphological and structural changes of C. albicans

The effect of Au NPs on the cell disruption and morphological changes were examined by FESEM analysis. Fig. 4(a)–(c) and (d)–(f) shows the lower and higher magnification FESEM images, respectively, of the control (untreated) and Au NPs treated *C. albicans.* The ultrastructural images of Au NPs treated *C. albicans* at the MIC (32 µg/mL) and MFC (64 µg/mL) levels showed notable morphological changes when compared to the control (Fig. 4(a) and (d)). At the MIC level (Fig. 4(b) and (e)) the cells showed surface deformities, while at the MFC level (Fig. 4(c) and (f)) there were clear cell destruction and cellular debris aggregation. Thus, the results revealed that the Au NPs causes cellular damage and destruction of the *C. albicans*, which correlates with the results of our previous studies of *C. albicans* cells after treatment with chitosan-metal (Ag and Au) nanocomposite at the MIC and MFC levels [47]. The quantitative elemental composition of the

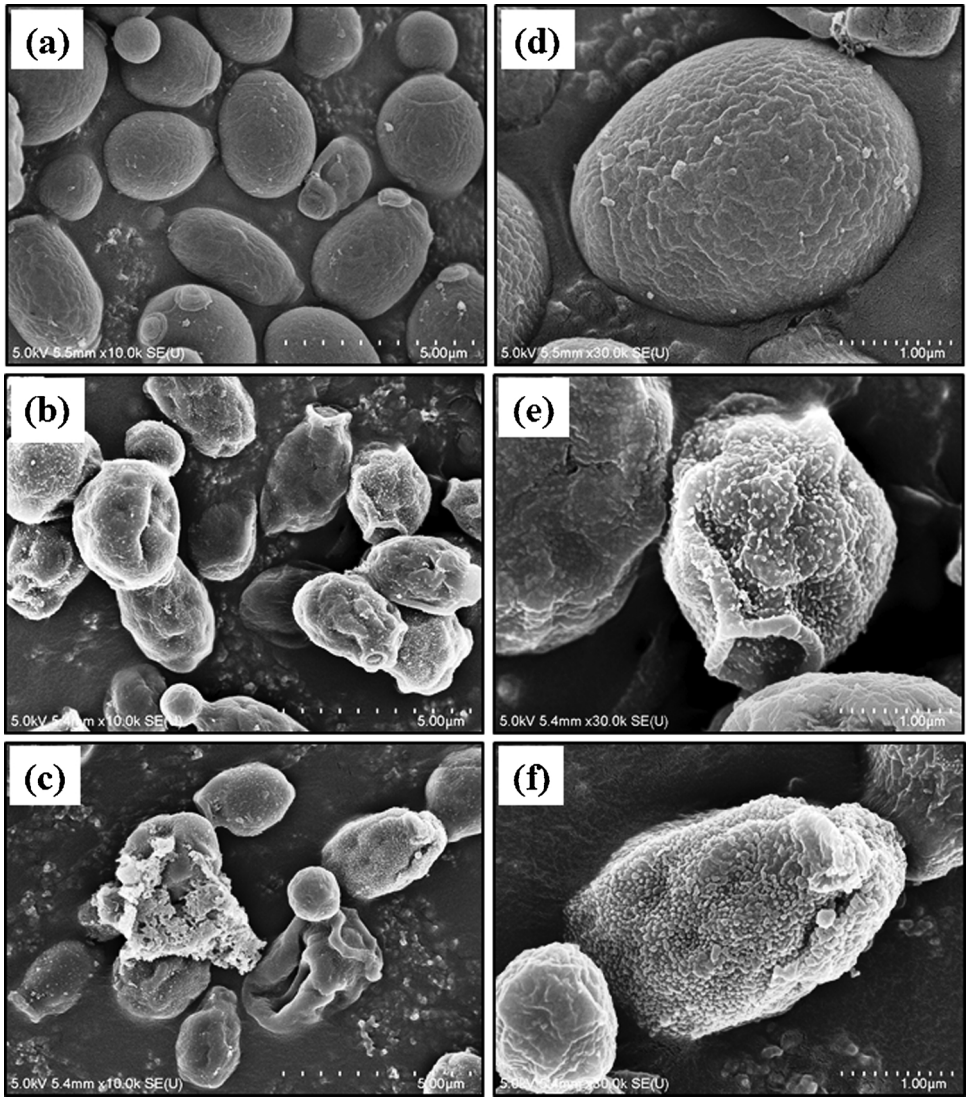

Fig. 4. Low- and High-magnification FESEM images of Au NPs treated *C. albican* (a, d) Control (untreated cells); Au NPs treated cells (b, e) 32 µg/mL and (c, f) 64.0 µg/mL.

control and the Au NPs treated *C. albicans* were analyzed by EDX coupled to an FESEM (Fig. 5). The results clearly showed the presence of Au on the membrane of *C. albicans* cells treated with Au NPs. The selected area of the EDX profile of *C. albicans* cell membrane (Fig. 5(b)) showed 1.23 % weight of Au, 42 % of Carbon (C), 31.99 % of oxygen (O) and total 24.38 % of other elements such as nitrogen (N) and phosphorous (P).

PI uptake assay was further performed to prove the cell membrane damage due to the Au NPs. Penetration of the PI into viable *C. albicans* cell is blocked by the cell membrane, while the damaged or dead cells easily allows the PI to penetrate into cells and subsequently stain the nucleus DNA to emit red fluorescence [26]. *C. albicans* cells were treated with Au NPs at the MIC and MFC levels, followed by PI staining. Non-treated control (Fig. 6(a)-(c)) did not show any fluorescence, indicating an intact cell wall structure. MIC (Fig. 6(d)-(f)) and MFC (Fig. 6(g)-(l)) treated cells displayed red fluorescence. Comparatively higher number of cells in the MFC treated sample was stained with PI and displayed intensified red fluorescence. Taken together, these results prove that the Au NPs damaged the cell membrane of *C. albicans* and subsequently caused cell death.

3.5. Safety assessment of Au NPs

Prior to the therapeutic application of Au NPs, biocompatibility of the synthesized Au NPs was tested with adult zebrafish and mammalian cells. The toxicity of Au NPs on zebrafish increased with increasing NPs concentrations. No fish mortality was observed in the control and for Au NPs treated groups with 12.5 and 25 µg/mL concentrations, indicating the nontoxic nature of Au NPs at lower concentrations. Further increase in the Au NPs concentration increased the fish mortality rate, and for 125 µg/mL Au NPs concentration 100 % fish mortality was observed. The LC_{50} of the synthesized Au NPs was found to be 62 µg/mL at 96 h exposure. R. Ramachandran et al. [48], reported an LC_{50} of 41 µg/mL for Au NPs synthesized using *Acalypha indica Linn,* which is far more toxic than the LC_{50} value found in the present work. The toxicity of NPs relied not only on the administered dose but also on the size, shape, capping agent, particle stability and the quality of the aquatic medium [49].

MTT assay was performed to assess the cell viability after 24 h treatment with different concentrations of Au NPs (0, 8, 16, 32, 64, 128 µg/mL) on HEK293T and A549 cells. The results (Fig. 7) showed that there was no significant difference ($P < 0.05$) in the cell viability up to 64 µg/mL of Au NPs concentrations compared to the control. At higher concentrations (128 µg/mL) slight toxicity was observed. Similar

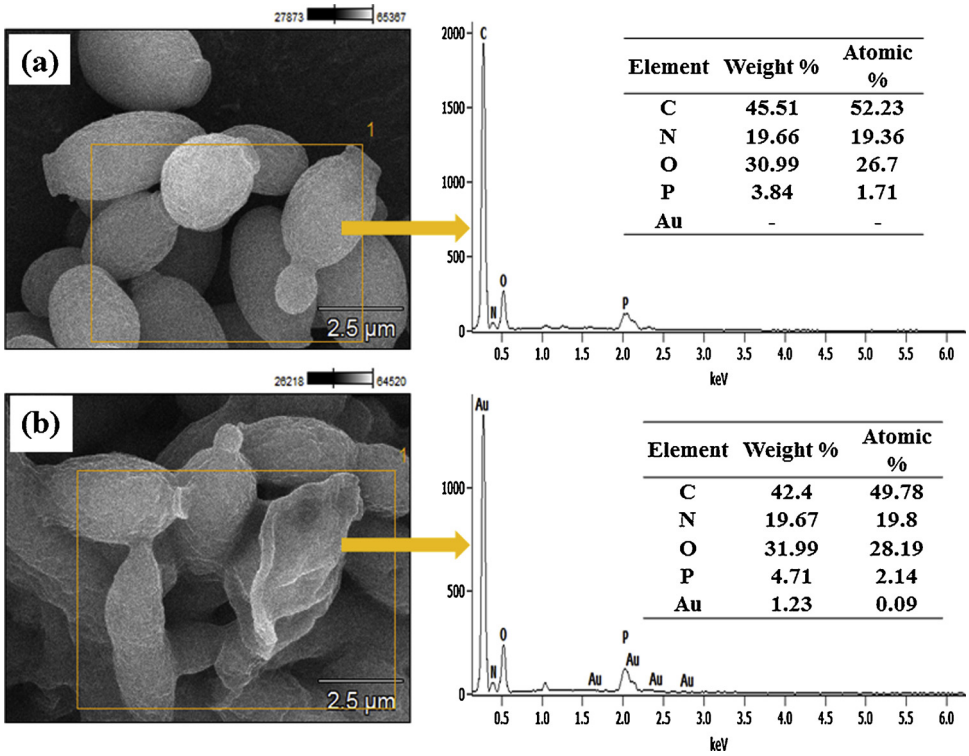

Fig. 5. FESEM image and EDX spectra of the (a) control, and (b) 32 µg/mL Au NPs treated *C. albicans* cells. The EDX spectra correspond to the selected area shown in the FESEM image.

cell viability was observed for HEK293-T cells after treatment with the Au NPs (0 − 100 µg/mL), which was synthesized using red seaweed *Gracilaria verrucosa* [50]. Also, the Au NPs synthesized using *Lonicera japonica* showed more than 95 % of cells viability on HEK293T cells at all tested concentrations (100 − 500 µg/mL) [51]. H. Sun et al., stated that the size, shape and surface properties of Au NPs play a key role on the ROS induced apoptosis and cell death [52]. Over all, the results of cell cytotoxicity of the present study showed no cytotoxic effect on the HEK293T and A549 cells at MIC (32 µg/mL) and MFC (64 µg/mL) level treatments. However, more experiments should be conducted to investigate the cell cytotoxic effect of Au NPs on other mammalian cells as well.

3.6. Efficacy of Au NPs therapy on C. albicans infection in zebrafish model

In vivo study was performed to examine the effect of green synthesized Au NPs on *C. albicans* replication in zebrafish. The zebrafish was developed as a model vertebrate host system for *C. albicans* infection studies [53]. Fish were injected with *C. albicans* cells into the dorsal muscle (Fig. 8(a)). At 72 hpi, PBS (negative control) applied injected site showed severe fungal growth (Fig. 8(b)) and fish displayed abnormal swimming behavior. The Au NPs (32 µg per fish) treated zebrafish showed less fungal growth at the injected site (Fig. 8(c)), which disappeared at 120 hpi (Data is not shown). However, no fungal growth was observed in Nystain (positive control) treated fish (Fig. 8(d)). With the infection, the cumulative survival rate at 120 hpi was 16 % and 66 % in the control and Au NPs treated groups, respectively. The highest survival rate of 74 % was observed for Nystain (10 µg per fish) treated group. However, there was a reduction of survival rate with the antifungal treatment, which may be attributed to the increased stress and side effects of the antifungals.

The localized filamentous growth of *C. albicans* in various anatomical sites, including the liver, gastrointestinal (GI) tract, connective tissue and muscle was observed in the dead fish with an infection dose of 1×10^8 CFU [54]. Similar observations of *C. albicans* colonization and filamentation at multiple locations have been reported in mouse model and human patients [55]. At 72 hpi, the histopathological analysis was carried out to detect the effect of Au NPs on the *C. albicans* hyphae and cells in zebrafish muscle. PBS treated fish had an extensive growth of *C. albicans* hypae and cells (Fig. 8(e)) compared to the Au NPs (Fig. 8(f)) and Nystain treated fish (Fig. 8(g)).Thus, the *in vivo* study results authenticated that the Au NPs exerts strong inhibition effects on the growth of *C. albicans* in zebrafish muscles. M.A. Sherwani et al., showed that the mixture of Au NPs conjugated to two different photosensitizers (methylene blue and toluidine blue O) significantly depleted the hyphal *C. albicans* burden against superficial skin and oral *C. albicans* infection in mice [56]. Similar histopathological observation was also obtained after the chitosan-gold nanocomposite treatment in *C. albicans* infected zebrafish [26].

3.7. Transcriptional response of immune gene in zebrafish upon C. albicans infection

To understand the host-pathogen interaction upon *C. albicans* infection and relevant treatments at molecular level, we determined the transcriptional responses of selected immune genes. The highest expression levels of all genes were reported in the infected control group, followed by Au NPs treated group and the least expression levels were observed in Nystatin treated group compared to PBS control (Fig. 9). Among the host-immune genes, the highest response of 35-fold was observed in *IL-1β* in infected control group, which was significantly reduced to 5-fold in Au NPs treated group and 2-fold in Nystatin treated positive control group. Similarly, *TNF-α, IL-6* and *IL-12* were highly upregulated (> 20 fold) in infected group and significantly reduced in treated groups. Moreover, chemokine, *Cxcl18b* was highly induced (10 fold) in non-treated control fish and reduced in both treatments. However, *IFN-γ* induction was not significant in control group and remained at basal levels in treatment groups.

During microbial infections, the pathogen-associated molecular patterns (PAMPs) were recognized and robust immune responses were

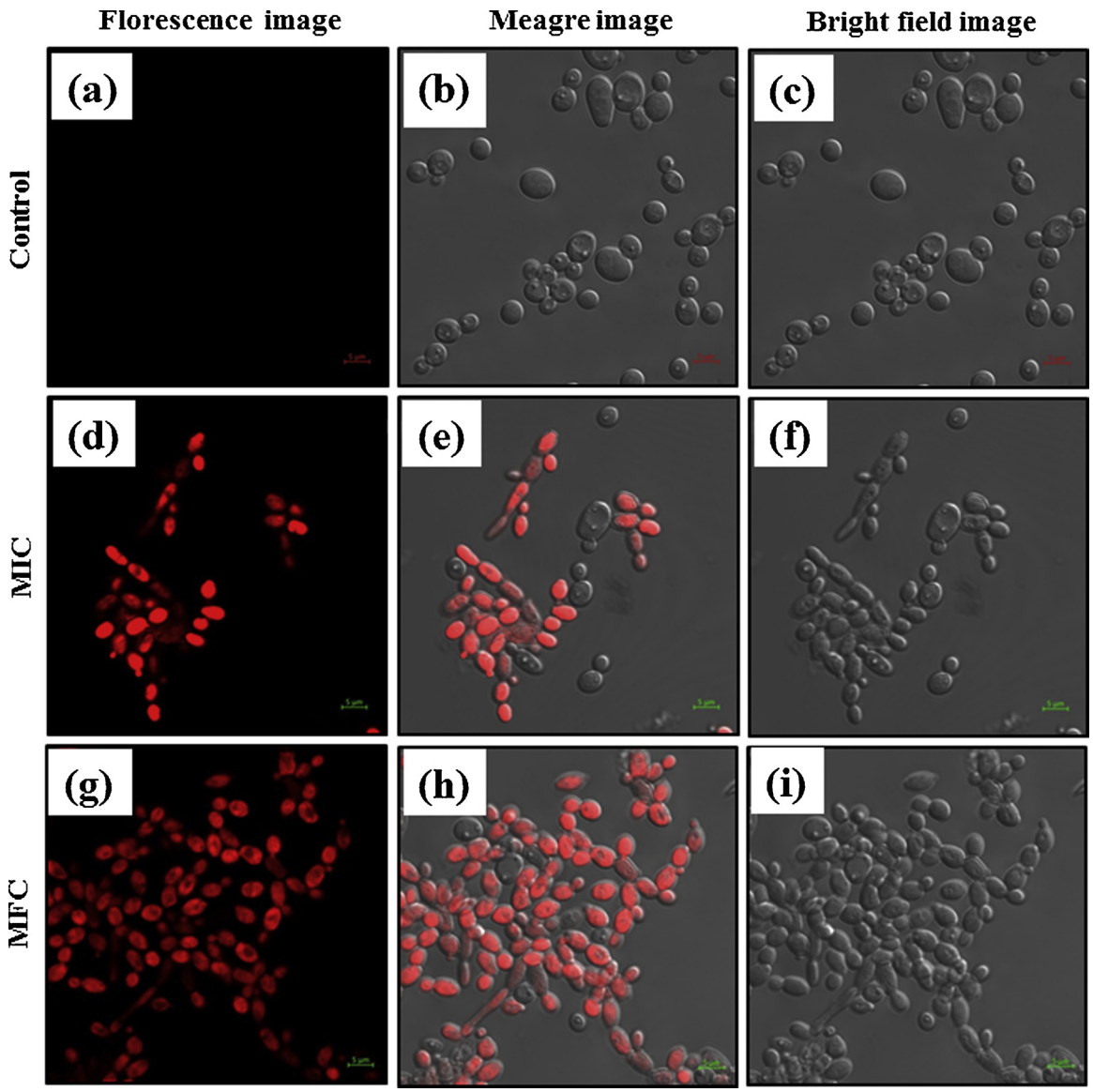

Fig. 6. CLSM image of Au NPs treated *C. albicans* cells. (a)-(c) control (untreated cells); (d)-(f) treated at MIC (32 μg/mL); and (g)-(i) treated at MFC (64 μg/mL).

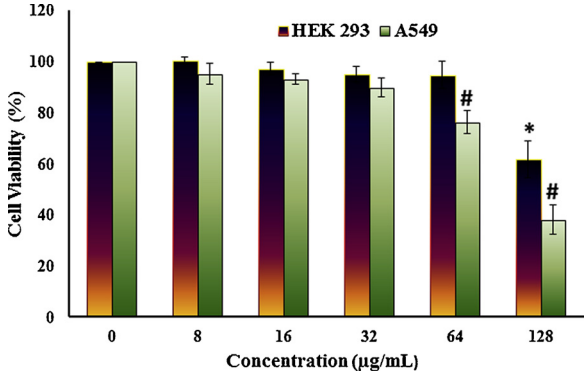

Fig. 7. Viability of mammalian cells (HEK293T and A549) after treatment Au NPs for different concentrations. Data are expressed as the mean ± SD ($n = 6$). The asterisk (*) and sharp (#) symbols indicates that the mean values are significantly different ($p < 0.05$) in HEK293T and A549 cells, respectively, between the control and the treated ones.

produced by host immune system. Consistent with the previous studies, pro-inflammatory cytokines such as *TNF-α, IL-1β* which are the targets of transcription factor *NF-κB* were highly up-regulated in zebrafish, suggesting that the immune response mechanism with candida infection may activate *IKK2/IκBα/NF-κB* signaling pathway [57]. Furthermore, *in vitro* studies with *C. albicans* infected gingival fibroblasts, demonstrated elevated *IL-6* and *IL-8* levels [58]. Chemokines which are associated with transporting immune cells to an infection site was highly up related in infected zebrafish muscle. The significant reduction of elevated cytokine expression due to Au NPs treatment indicates the positive effects of Au NPs against pathogen.

4. Conclusion

Au NPs was successfully green synthesized using *SP* extract from *S. maxima* without the addition of chemical reducing agent. The MIC and MFC values of the green synthesized Au NPs were 32 and 64 μg/mL, respectively. The results of the growth curve, cell viability and PI uptake analysis revealed the concentration dependent effect of Au NPs on *C. albicans*. Further, *in vivo* results revealed that *C. albicans* could invade the muscle tissue of the zebrafish at tested concentration. It has been proven that Au NPs treatment in constant time intervals could inhibit

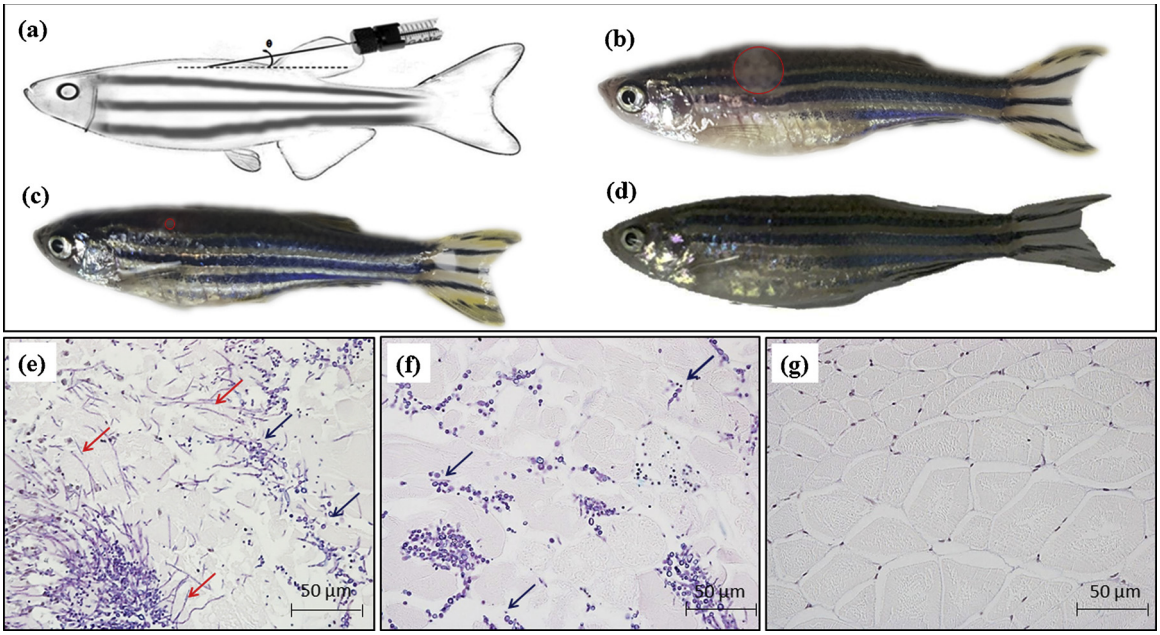

Fig. 8. Efficacy of Au NPs therapy on *C. albicans* infection in zebrafish dorsal muscle at 72 hpi. (a) Schematic diagram of *C. albicans* injection with 15° angle. (b) Control; (c) Au NPs treated fish; (D) Nystatin treated fish. Histopathological examination of *C. albicans* infection in zebrafish dorsal muscle tissue, the infected site showed the invading yeast-hyphae and inflamed tissues with cell infiltration (×400). (e) Control; (f) Au NPs treated fish tissue; (g) Nystatin treated fish tissue. The red and blue arrows indicate *C. albicans* hyphae and cells, respectively (For interpretation of the references to colour in this figure legend, the reader is referred to the web version of this article).

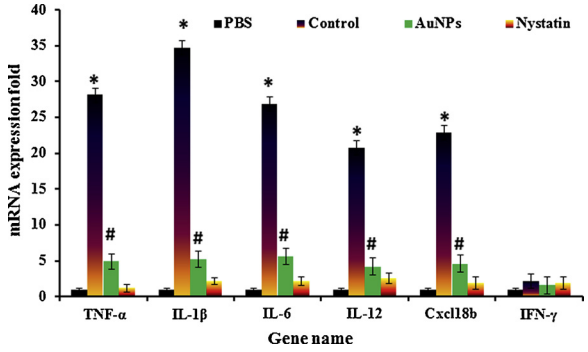

Fig. 9. Transcriptional responses of host defense and inflammatory genes in co-infected and healthy zebrafish muscle tissue. Relative mRNA expression fold was analyzed according to the Livak method ($2\text{-}\Delta\Delta^{CT}$) using the zebrafish β-actin as a house keeping gene. Data are expressed as mean ± SD ($n = 3$). The asterisk (*) symbol indicate that the mean values are significantly different ($p < 0.05$) between PBS-injected control group and the *C. albicans* infected untreated group. The sharp (#) symbol indicates that the mean values are significantly different ($p < 0.05$) between the Au NPs treated and PBS-injected control group.

the fungal growth and increase the survival rate of zebrafish. Non-treated fish infected with *C. albicans* showed higher relative mRNA expression levels of inflammatory cytokines in zebrafish muscle tissue than the Au NPs treat infected fish. The green synthesized Au NPs showed no cytotoxic effect on HEK293T and A549 mammalian cells. The results demonstrate that the green synthesized Au NPs possesses good biocompatibility and exhibits potent anticandidal activity.

CRediT authorship contribution statement

S.H.S. Dananjaya: Formal analysis, Investigation, Writing - original draft. **N.T. Thu Thao:** Formal analysis, Investigation. **H.M.S.M. Wijerathna:** Formal analysis, Investigation. **Jisoo Lee:** Formal analysis, Investigation. **M. Edussuriya:** Resources, Writing - review & editing. **Dongrack Choi:** Investigation, Resources, Supervision. **R. Saravana Kumar:** Conceptualization, Resources, Supervision, Writing - review & editing.

Declaration of Competing Interest

The authors declare that they have no known competing financial interests or personal relationships that could have appeared to influence the work reported in this paper.

Acknowledgements

Part of this work was supported by the Faculty research grant of Faculty of Science, University of Ruhuna (RU/SF/RP/2018/06), Sri Lanka. We greatly appreciate the technicians from National NanoFab Center (NNFC), Korea Advanced Institute of Science and Technology for their technical assistance.

References

[1] M.A. Affan, D.W. Lee, S.M. Al-Harbi, H.J. Kim, N.I. Abdulwassi, S.J. Heo, C. Oh, H.S. Park, C.W. Ma, H.Y. Lee, D.H. Kang, Variation of *Spirulina maxima* biomass production in different depths of urea-used culture medium, Braz. J. Microbiol. 46 (2015) 991–1000.
[2] F. Kurd, V. Samavati, Water soluble polysaccharides from *Spirulina platensis*: extraction and *in vitro* anti-cancer activity, Int. J. Biol. Macromol. 74 (2015) 498–506.
[3] S.Y. Xu, X. Huang, K.L. Cheong, Recent advances in marine algae polysaccharides: isolation, structure, and activities, Mar. Drugs 15 (2017) E388.
[4] H.Q. Zhang, A.P. Lin, Y. Sun, Y.M. Deng, Chemo- and radioprotective effects of polysaccharide of *Spirulina platensis* on hemopoietic system of mice and dogs, Acta Pharmacol. Sin. 22 (2001) 1121–1124.
[5] M. Rasool, E.P. Sabina, Appraisal of immunomodulatory potential of *Spirulina fusiformis*: an in vivo and in vitro study, J. Nat. Med. 63 (2009) 169–175.
[6] C.A. Ovando, J.C. De Carvalho, G.V.De.M. Pereira, P. Jacques, V.T.S. Soccol, C.R. Soccol, Functional properties and health benefits of bioactive peptides derived from Spirulina: a review, Food Rev. Int. 34 (2016) 34–51.
[7] A. Mizera, M. Kuczaj, A. Szul, Impact of the *Spirulina maxima* extract addition to semen extender on bovine sperm quality, Ital. J. Anim. Sci. 18 (2019) 601–607.
[8] M.P. Patil, G.D. Kim, Marine microorganisms for synthesis of metallic nanoparticles and their biomedical applications, Colloids Surf. B Biointerfaces 172 (2018) 487–495.
[9] C. Wang, X. Gao, Z. Chen, Y. Chen, H. Chen, Preparation, characterization and

application of polysaccharide-based metallic nanoparticles: a Review, Polymers (Basel) 9 (2017) E689.
[10] A.K. Singh, R. Tiwari, V.K. Singh, P. Singh, Sk.R. Khadim, U. Singh, Laxmi, V. Srivastava, S.H. Hasan, R.K. Asthana, Green synthesis of gold nanoparticles from *Dunaliella salina*, its characterization and *in vitro* anticancer activity on breast cancer cell line, J. Drug Deliv. Sci. Tec. 51 (2019) 164–176.
[11] G. Oza, S. Pandey, A. Mewada, G. Kalita, M. Sharon, Facile biosynthesis of gold nanoparticles exploiting optimum pH and temperature of fresh water algae *Chlorella pyrenoidusa*, Adv. Appl. Sci. Res. 3 (2012) 1405–1412.
[12] L. Li, Z. Zhang, Biosynthesis of gold nanoparticles using green alga *Pithophora oedogonia* with their electrochemical performance for determining carbendazim in soil, Int. J. Electrochem. Sci. 11 (2016) 4550–4559.
[13] A.U. Khan, M. Khan, N. Malik, M.H. Cho, M.M. Khan, Recent progress of algae and blue-green algae-assisted synthesis of gold nanoparticles for various applications, Bioprocess Biosyst. Eng. 42 (2019) 1–15.
[14] K.S. Suganya, K. Govindaraju, V.G. Kumar, T.S. Dhas, V. Karthick, G. Singaravelu, M. Elanchezhiyan, Blue green alga mediated synthesis of gold nanoparticles and its antibacterial efficacy against Gram positive organisms, Mater. Sci. Eng., C. 47 (2015) 351–356.
[15] M.F. Lengke, M.E. Fleet, G. Southam, Morphology of gold nanoparticles synthesized by filamentous cyanobacteria from gold (I)-thiosulfate and gold (III)-chloride complexes, Langmuir 22 (2006) 2780–2787.
[16] E. de Alteriis, V. Maselli, A. Falanga, S. Galdiero, F.M. Di Lella, R. Gesuele, M. Guida, E. Galdiero, Efficiency of gold nanoparticles coated with the antimicrobial peptide indolicidin against biofilm formation and development of *Candida* spp. clinical isolates, Infect. Drug Resist. 11 (2018) 915–925.
[17] V. Manohar, C. Ingram, J. Gray, N.A. Talpur, B.W. Echard, D. Bagchi, H.G. Preuss, Antifungal activities of origanum oil against *Candida albicans*, Mol. Cell. Biochem. 228 (2001) 111–117.
[18] W. Lee, D.G. Lee, A novel mechanism of fluconazole: fungicidal activity through dose-dependent apoptotic responses in *Candida albicans*, Microbiology 164 (2018) 194–204.
[19] M.A. Benavent, S. Wang, R. Mateos, B. Sarria, L. Bravo, Antiproliferative and cytotoxic effects of green coffee and yerba mate extracts, their main hydroxycinnamic acids, methylxanthine and metabolites in different human cell lines, Food Chem. Toxicol. 106 (2017) 125–138.
[20] S. Galdiero, A. Falanga, R. Berisio, P. Grieco, G. Morelli, M. Galdiero, Antimicrobial peptides as an opportunity against bacterial diseases, Curr. Med. Chem. 22 (2015) 1665–1677.
[21] Q. Liu, C. Yao, Y. Sun, W. Chen, H. Tan, X. Cao, S. Xue, H. Yin, Production and structural characterization of a new type of polysaccharide from nitrogen-limited *Arthrospira platensis* cultivated in outdoor industrial-scale open raceway ponds, Biotechnol. Biofuels 12 (2019) 131.
[22] R. Chaiklahan, N. Chirasuwan, P. Triratana, V. Loha, S. Tia, B. Bunnag, Polysaccharide extraction from *Spirulina* sp. and its antioxidant capacity, Int. J. Biol. Macromol. 58 (2013) 73–78.
[23] Ede M. Castro, E. Shannon, N. Abu-Ghannam, Effect of fermentation on enhancing the nutraceutical properties of *Arthrospira platensis* (Spirulina), Fermentation 5 (2019) 28.
[24] P. Capek, E. Machová, J. Turjan, Scavenging and antioxidant activities of immunomodulating polysaccharides isolated from *Salvia officinalis* L, Int. J. Biol. Macromol. 44 (2009) 75–80.
[25] I. Kumar, M. Mondal, V. Meyappan, N. Sakthivel, Green one-pot synthesis of gold nanoparticles using *Sansevieria roxburghiana* leaf extract for the catalytic degradation of toxic organic pollutants, Mater. Res. Bull. 117 (2019) 18–27.
[26] S.H.S. Dananjaya, R.M.C. Udayangani, C. Oh, C. Nikapitiya, J. Lee, M. De Zoysa, Green synthesis, physio-chemical characterization and anti-candidal function of a biocompatible chitosan gold nanocomposite as a promising antifungal therapeutic agent, RSC Adv. 7 (2017) 9182–9193.
[27] OECD, Test No. 203: Fish, Acute Toxicity Test, OECD Publishing, Paris, 1992.
[28] S.H.S. Dananjaya, R.S. Kumar, M. Yang, C. Nikapitiya, J. Lee, M. De Zoysa, Synthesis, characterization of ZnO-chitosan nanocomposites and evaluation of its antifungal activity against pathogenic Candida albicans, Int. J. Biol. Macromol. 108 (2018) 1281–1288.
[29] A.M. da Rocha, L.W. Kist, E.A. Almeida, D.G.H. Silva, C.D. Bonan, S. Altenhofen, C.G. Kaufmann Jr, M.R. Bogo, D.M. Barros, S. Oliveira, V. Geraldo, R.G. Lacerda, A.S. Ferlauto, L.O. Ladeira, J.M. Monserrat, Neurotoxicity in zebrafish exposed to carbon nanotubes: effects on neurotransmitters levels and antioxidant system, Comp. Biochem. Physiol. C Toxicol. Pharmacol. 218 (2019) 30–35.
[30] K. Livak, T. Schmittgen, Analysis of relative gene expression data using real time quantitative PCR and the $2^{-\Delta\Delta Ct}$ method, Methods 25 (2001) 402–408.
[31] H. Ma, H. Xiong, X. Zhu, C. Ji, J. Xue, R. Li, B. Ge, H. Cui, Polysaccharide from *Spirulina platensis* ameliorates diphenoxylate-induced constipation symptoms in mice, Int. J. Biol. Macromol. 133 (2019) 1090–1101.
[32] M.S. Attia, G.S. El-Sayyad, S.S. Saleh, M.B. Naglaa, A.I. El-Batal, Spirulina platensis-polysaccharides promoted green silver nanoparticles production using gamma radiation to suppress the expansion of pear fire blight-producing Erwinia amylovora, J. Clust. Sci. 30 (2019) 919–935.
[33] G.A. Filip, B. Moldovan, I. Baldea, D. Olteanu, R. Suharoschi, N. Decea, C.M. Cismaru, E. Gal, M. Cenariu, S. Clichici, L. David, UV-light mediated green synthesis of silver and gold nanoparticles using Cornelian cherry fruit extract and their comparative effects in experimental inflammation, J. Photochem. Photobiol. B 191 (2019) 26–37.
[34] P.M. Njana, M.R. Bindhu, R.B. Rakhi, Green synthesized gold nanoparticle dispersed porous carbon composites for electrochemical energy storage, Mater. Sci. Energy Technol. 2 (2019) 389–395.
[35] X. Chen, X. Zhao, Y. Gao, J. Yin, M. Bai, F. Wang, Green synthesis of gold nanoparticles using Carrageenan oligosaccharide and their *in vitro* antitumor activity, Mar. Drugs 16 (2018) 277.
[36] N. Yang, W.H. Li, Preparation of gold nanoparticles using chitosan oligosaccharide as a reducing and capping reagent and their in vitro cytotoxic effect on Human fibroblasts cells, Mater. Lett. 138 (2015) 154–157.
[37] D. Wang, J.F.C. Loo, J. Chen, Y. Yam, S.C. Chen, H. He, S.K. Kong, H.P. Ho, Recent advances in surface plasmon resonance imaging sensors, Sensors Basel (Basel) 19 (2019) 1266.
[38] J. Nellore, P.C. Pauline, K. Amarnath, Biogenic synthesis by *Sphearanthus amaranthoids*; towards the efficient production of the biocompatible gold nanoparticles, Dig. J. Nanomater. Bios. 7 (2012) 123–133.
[39] A. Gupta, S. Mumtaz, C.H. Li, I. Hussain, V.M. Rotello, Combatting antibiotic-resistant bacteria using nanomaterials, Chem. Soc. Rev. 48 (2019) 415–427.
[40] S. Chaicherd, M.C. Killingsworth, D. Pissuwan, Toxicity of gold nanoparticles in a commercial dietary supplement drink on connective tissue fibroblast cells, SN Appl. Sci. 1 (2019) 336.
[41] M.N. Nadagouda, R.S. Varma, Green synthesis of silver and palladium nanoparticles at room temperature using coffee and tea extract, Green Chem. 10 (2008) 859–862.
[42] L.R. Peixoto, P.L. Rosalen, I.A. Ferreira, F.G. De Carvalho, L.R. Castellano, R.D. De Castro, Antifungal activity, mode of action and anti-biofilm effects of *Laurus nobilis* Linnaeus essential oil against *Candida* spp, Arc. Oral Biol. 73 (2017) 179–185.
[43] M. Seong, D.G. Lee, Reactive oxygen species-independent apoptotic pathway by gold nanoparticles in Candida albicans, Microbiol. Res. 207 (2018) 33–40.
[44] S. Khan, F. Alam, A. Azam, A.U. Khan, Gold nanoparticles enhance methylene blue-induced photodynamic therapy: a novel therapeutic approach to inhibit *Candida albicans* biofilm, Int. J. Nanomedicine 7 (2012) 3245–3257.
[45] A. Jebali, F.H.E. Hajjar, S. Hekmatimoghaddam, B. Kazemi, J.M. De La Fuente, M. Rashidi, Triangular gold nanoparticles conjugated with peptide ligands: a new class of inhibitor for *Candida albicans* secreted aspartyl proteinase, Biochem. Pharmacol. 90 (2014) 349–355.
[46] F.H.E. Hajjar, A. Jebali, S. Hekmatimoghaddam, The inhibition of *Candida albicans* secreted aspartyl proteinase by triangular gold nanoparticles, Nanomed. J. 2 (2015) 54–59.
[47] D.C.M. Kulatunga, S.H.S. Dananjaya, G.I. Godahewa, J. Lee, M. De Zoysa, Chitosan silver nanocomposite (CAgNC) as an antifungal agent against *Candida albicans*, Med. Mycol. 55 (2017) 213–222.
[48] R. Ramachandran, C. Krishnaraj, V.K.A. Kumar, S.L. Harper, T.P. Kalaichelvan, S.I. Yun, In vivo toxicity evaluation of biologically synthesized silver nanoparticles and gold nanoparticles on adult zebrafish: a comparative study, Biotech. 8 (2018) 8.
[49] K. Bilberg, M.B. Hovgaard, F. Besenbacher, E. Baatrup, In vivo toxicity of silver nanoparticles and silver ions in zebrafish (*Danio rerio*), J. Toxicol. (2012) 293784.
[50] C. Chellamuthu, R. Balakrishnan, P. Patel, R. Shanmuganathan, A. Pugazhendhi, K. Ponnuchamy, Gold nanoparticles using red seaweed *Gracilaria verrucosa*: Green synthesis, characterization and biocompatibility studies, Process Biochem. 80 (2019) 58–63.
[51] M.P. Patil, L.L.A. Piad, E. Bayaraa, P. Subedi, N.H. Tarte, G.D. Kim, Doxycycline hyclate mediated silver-silver chloride nanoparticles and their antibacterial activity, J. Nanostruct. Chem. 9 (2019) 53–60.
[52] H. Sun, J. Jia, C. Jiang, S. Zhai, Gold nanoparticle-induced cell death and potential applications in nanomedicine, Int. J. Mol. Sci. 19 (2018) E754.
[53] D.C.M. Kulatunga, S.H.S. Dananjaya, C. Nikapitiya, C.H. Kim, J. Lee, M. De Zoysa, Candida albicans infection model in Zebrafish (Danio rerio) for screening anticandidal drugs, Mycopathologia 184 (2019) 559–572.
[54] C.C. Chao, P.C. Hsu, C.F. Jen, I.H. Chen, C.H. Wang, H.C. Chan, P.W. Tsai, K.C. Tung, C.H. Wang, C.Y. Lan, Y.J. Chuang, Zebrafish as a model host for Candida albicans infection, Infect. Immun. 78 (2010) 2512–2521.
[55] F.C. Odds, Candidaand candidosis: a review and bibliography, J. Basic Microbiol. 30 (1988) 382–383.
[56] M.A. Sherwani, S. Tufail, A.A. Khan, M. Owais, Gold nanoparticle-Photosensitizer conjugate based photodynamic inactivation of biofilm producing cells: potential for treatment of *C. albicans* infection in BALB/c mice, PLoS One 10 (2015) e0131684.
[57] V. Muller, D. Viemann, M. Schmidt, N. Endres, S. Ludwig, M. Leverkus, J. Roth, M. Goebeler, Candida albicans triggers activation of distinct signaling pathways to establish a proinflammatory gene expression program in primary human endothelial cells, J. Immunol. 179 (2007) 8435–8445.
[58] A. Dongari-Bagtzoglou, K. Wen, I.B. Lamster, Candida albicans triggers interleukin-6 and interleukin-8 responses by oral fibroblasts in vitro, Oral Microbiol. Immunol. 14 (1999) 364–370.